Graphene oxide decorated Tin sulphide quantum dots for electrochemical detection of dopamine and tyrosine

M. Hasheena
A. Ratnamala
M. Noorjahan
G. Deepthi Reddy
Shiprath K
Manjunatha H
Chandra Babu Naidu K (chandrababu954@gmail.com)
GITAM University - Bengaluru Campus https://orcid.org/0000-0002-0580-6383

Research Article

Keywords: GO-SnS2 quantum dots, dopamine, tyrosine, graphene oxide, electrochemical

Posted Date: April 12th, 2022

DOI: https://doi.org/10.21203/rs.3.rs-1532467/v1

Abstract

The current study highlights the design and construction of a sensitive and selective sensor for detection of dopamine and tyrosine using a GO-SnS_2 quantum dots by a drop casting method on glassy carbon electrode. Highly porous nano-crystalline GO-SnS_2 quantum dots were synthesized by using ultrasonication followed by hydrothermal method in a facile manner. XRD, SEM, XPS, TEM, and pore size distribution techniques were used to characterize the quantum dots that were produced. The newly fabricated electrode was evaluated for EIS (Electrochemical impedance spectroscopy), CV (cyclic voltammetry) and chronoamperometric methods. The observed limit of detection of dopamine was observed to be 26 nM. High selectivity and sensitivity were observed for electrochemical detection of dopamine and tyrosine.

Introduction

Dopamine and tyrosine are essential biomolecules which play a key role in human metabolism. Tyrosine is an important precursor of thyroid hormones, dopamine, adrenaline, and other hormones that are used to establish and maintain a proper balance in humans [1]. Hypothyroidism, hypochondria, and dementia are all caused by a lack of tyrosine. Dopamine belongs to the catecholamine family and is formed in the brain by dopaminergic neurons [2]. Dopamine is a key signal-transmission component between neurons because it is linked to the majority of important human body functions like motor control, reward, motivation, and cognition [3–6]. Low levels of dopamine and tyrosine in the blood, as well as the death of dopaminergic neurons in the brain, have been linked to a range of significant neurological illnesses, including Parkinson's disease, psychosis, and attention deficit hyperactivity disorder (ADHD) drug addiction [6, 7]. To solve this problem, several studies have described novel approaches for detecting dopamine and tyrosine in a highly sensitive and selective manner, which might be utilized to identify dopamine and tyrosine-related neurological illnesses promptly [8–10].

Because of its short detection time and cost efficiency, the electrochemical sensing approach is recognized as one of the most effective approaches for dopamine and tyrosine detection among the different existing methods such as ELISA, colorimetric methods, Raman, and HPLC. [11–14]. Dopamine and tyrosine are redox-active chemicals that may be reduced or oxidized at different potentials, and their electrical characteristics can be used to detect their presence in a sample (usually human blood). The use of an electrochemical dopamine and tyrosine detection approach is challenging due to signal interference from other biological molecules (e.g., uric acid (UA), ascorbic acid (AA), and catecholamine molecules). Signal interference might greatly limit the sensitivity of dopamine detection since the reduction and oxidation potentials of these biological substances allegedly coincide with those of dopamine [15–17]. Furthermore, the electrochemical sensitivity of dopamine is still lower than that of other traditional techniques like HPLC and ELISA, which is a substantial hurdle to overcome before this approach can be utilized to detect accurate levels of dopamine [18]. By functionalizing electrode surfaces or introducing other types of conductive materials, several attempts have been made to overcome the issues of selectivity and sensitivity.

Graphene, a two-dimensional (2D) honeycomb structure made up of pure carbon molecules, has been widely exploited in different scientific fields, including batteries, display panels, solar cells, and even biological applications [19–22]. Furthermore, graphene derivatives have been shown to exhibit notable dopamine-detection properties [23], which are principally owing to – and electrostatic interactions between the graphene oxides' surfaces. Various graphene-derivative-modified electrodes have been created to increase the performance of dopamine biosensors, including graphene/glassy carbon electrode (GCE), graphene–gold nanoparticles/GCE, TiO2–graphene/GCE, and GO/GCE electrodes [24–27]. One of the most intriguing carbonaceous compounds is graphene, a one-layer thick sheet with exceptional optical, thermal, and electrical characteristics. The discovery of porous graphene oxide (PGO), a type of graphene-oxide sheet with numerous hydroxyl groups and a porous surface [28], has the potential to improve the electrostatic interaction between the PGO and the analytes while also facilitating electron transfer between the molecules and the underlying electrode substrates [29].

Among the various binary compounds of tin chalcogenides, tin sulphides are well studied or explored owing to adaptable chemical nature and can be fabricated into hybrids, composites, non-toxic nature etc. hence they are widely used in energy storage devices, solar cells and optoelectronic devices. Despite this, the electrochemical procedure produces substantial capacity fading in tin sulphides due to the high-volume change. [14–16]. Because these matrices can greatly promote electron/ion transfer and effectively accommodate cycle-induced stress/strain of SnS, the electrochemical performance of tin sulphide has recently been improved by grafting nanosized tin sulphide into various types of carbon matrices (e.g., carbon spheres, amorphous carbon, macroporous carbon, carbon nanotubes, or graphene) [17–23]. Despite considerable gains in gravimetric capacity and cycle performance, the nanostructure of these composites, in combination with the low tap density of carbon matrix, can restrict volumetric capacity [24, 25]. Furthermore, the creation of these composites typically involves severe conditions or sophisticated synthesis, both of which are costly to industry. As a result, achieving a simple, scalable synthesis of tin sulphide-based graphene materials with superior volumetric storage remains a major challenge.

We used a facile hydrothermal method to create a novel graphene Oxide/ SnS_2 (GO-SnS_2) composite. SnS_2 quantum dots are tightly supported on porous graphene oxide (PGO) in the composite, forming a primary microstructure and then assembling into a secondary nanostructure. The tap density of the nanostructured SnS_2 and PGO hybrid is very high. The combination of SnS_2 quantum dots and PGO nanosheets inside nanosized building blocks can not only improve overall electron/ion transport, but also efficiently insert SnS_2 volume change and provide strong structural stability to the composite. As a result, the tightly compacted GO-SnS_2 quantum dots show high, fast, and stable dopamine electrochemical detection. Thus, the prepared GO-SnS_2 quantum dots were found to be exhibiting superior electrochemical performance, combined with its simple scalable synthesis, makes it a promising candidate for practical application.

Experimental Section

2.1. Reagents and Chemicals

Stannous dichloride ($SnCl_2.4H_2O$), Sodium Sulphide flakes (make: SD fine chemicals, INDIA), Dopamine (make: Aldrich), Tyrosine from Fischer Scientific Ltd., Potassium ferrocyanide and Potassium Chloride from SD Fine. Chemicals used in this work are of AR grade or analytical grade and used as received.

2.2. Synthesis of SnS_2 nanoparticles using plant extract

Fresh *Syzigium cumini* (*S. cumini*) leaves (100g) were collected and rinsed several times with distilled water to remove foreign particles before being ground using a mortar and pestle. The combination is placed in a beaker with distilled water, agitated for half an hour to ensure equal dispersion throughout the medium, and then filtered using Whatman filter paper to get pure *S. cumini* extract. The crude extract was diluted with distilled water before being kept in airtight bottles in the refrigerator.

SnS_2 quantum dot composites were made by dissolving a 0.1M solution of $SnCl_2.4H_2O$ in 250 ml of heated *S. cumini* leaf extract and shaking it. After 5 minutes, the Na_2S solution was added drop by drop, and the solution became yellow after 30 minutes of stirring. To get the SnS_2 -nanoparticles, the resultant solid is centrifuged and washed with water, ethanol, then kept in an oven for drying at 60°C for about 8 hours.

2.3. Synthesis of Graphene oxide/SnS_2 Nanocomposites (NCs)

Ultra-sonication followed by the hydrothermal method is simple and fast for synthesis of graphene oxide/ SnS_2 nanocomposite materials. In a beaker about 500 mg of graphene oxide in 100-ml water are homogenized by using an ultrasonic bath. The homogenous graphene solution in the beaker were mixed with preformed SnS_2 synthesized, followed by hydrothermal treatment for 24 h at 100 ^{0}C without adding any precipitating agent. The resultant colloidal solution was rinsed with ethanol and water, and then aged for roughly 12 hours in beaker. Finally, the resultant combination solutions were dried in an oven at 65°C for 24 hours, yield GO-SnS_2 quantum dots.

2.4. Fabrication of electrode

Before being utilised to form the working electrode, the glassy carbon electrode (GCE) was thoroughly washed with deionized water and polished with an alumina polishing pad. The material was sonicated for 15 minutes after being distributed in 1 mL DMF. To make a thin layer, the resultant mixture was drop casted over the surface of GCE with a micropipette and air dried overnight at room temperature.

3.0. Material Characterization:

The produced GO-SnS_2 quantum dots were examined using a various of characterization methods. The size of GO-SnS_2 quantum dot phase purity and crystalline nature were examined using the X'pert Pro X-ray diffractometer with Ni filtered Cu K radiation (= 1.5406, 2 = 0–60). SEM (ZEISS EVO 18 model) was

used to record the morphology of the GO-SnS_2 quantum dots.The GO-SnS_2 quantum dots were photographed and their selected area electron diffraction (SAED) patterns were obtained using an FEI TECHNAI G2 transmission electron microscope (TEM). A UV-1800 pc Shimadzu spectrophotometer was used to detect colloidal dispersions of GO-SnS2 quantum dots in 200 to 1100 nm range (0.001M). X-ray photoemission spectra were obtained on a KRATOS AXIS 165 with Mg K radiation (1253.6 eV) at 75 W. The C 1s line at 284.6 eV was utilized as an internal reference. Asymmetric gaussian forms were adopted in each situation. Binding energies of similar samples were typically constant within 0.1 eV.

Results And Discussion

4.1 Material Characterization

4.1.1 XRD

The crystal structure of the as synthesized GO-SnS_2 quantum dots was given in Fig. 1. The diffraction peaks at 2θ = 26.0 and also a hump around 25 shows the sp^2 graphene carbon.

The peaks observed at 2θ = 27.0 (100), 34.09(101), 42.58(102), 51.8(111), 59.14(200) and its corresponding planes is attributed to the hexagonal phase of SnS_2 [31]. The diffraction patterns agree well with the JCPDS card No. 23–0677. The obtained peaks are sharp with no impurities. The particle size calculated based on Scherrer's equation at 2θ = 26.0, 34.09 and 42.58 are estimated to be 5.27 nm, 9.19 nm and 7.74 nm respectively.

4.1.2 XPS

The oxidation statesandsurface chemical functionalities were examined by using XPS spectra. XPS patterns of C1s shows a prominent peak at binding energy of 284.78eV which refer to sp^2 graphitic carbon and shown in fig. 2a. As given in fig. 2b showing the high-resolution Sn 3d spectra with two peaks at Sn $3d_{5/2}$ (487.98 eV) and Sn $3d_{3/2}$ (496.28 eV) with a 9.3 eV energy gap, suggesting the presence of Sn^{4+} as the main phase present in the material. The SnS phase was not detected in the SnS_2–GO XRD patterns, as previously stated. [32].

4.1.3 Pore size distribution

Figure 3 (a), (b) and (c) depicts the N_2 adsorption and desorption isotherms of GO-SnS_2 quantum dots. As observed from the Fig. 3c, the adsorption isotherms are similar to that of type (IV) isotherms with prominent hysteresis loop in the P/P0 range of 0.5-1 reflecting the presence of mesopores. The synthesized GO-SnS_2 quantum dots showing the mesoporosity and is further confirmed by corresponding pore size distribution [33]. The SnS_2-GO quantum dots have a surface area of 13.865 m^2/g, an average pore size of 15.24 nm, and a measured pore volume of 0.066 cc/g. The findings are consistent with previous reported results [33].

4.1.4. SEM and TEM

Figure 4 (a) and (b) shows the SEM and TEM images of synthesized GO-SnS_2 quantum dots. The SEM pictures disclose that the particles are agglomerated with sheet like morphology of the graphene on which the SnS_2 particles are decorated and the sheets are attached to each other due to tiny dimensions and large surface energy. Each nano-cluster size ranges from, 31.40–57.83 nm, as indicated from SEM images. The SnS_2 particles were seem to be embedded in the grapheme sheets [34]. The EDAX patterns are given in Fig. 4(c) and the surface composition of C, O, Sn and S are in a specific area are 82.05, 15.78, 1.84 and 0.32 (atomic weight percent) respectively.

The TEM images of GO-SnS_2 in Fig. 4b, demonstrates the quantum dots of size around 3 nm. The quantum dots are showing good crystallinity and the SAED pattern (Fig. 4d) infringes with hexagonal phase of tin sulphide and SnS_2 phases were decorated on graphene oxide, which is well in accordance with that of XRD.

4.2 Electrochemical performance of dopamine and tyrosine on the SnS_2 -GO nanocomposite modified electrode

Dopamine and tyrosine coexist in blood and many biological fluids and interfere with each other in the detection and moreover the concentration of tyrosine is generally low. High concentration of DA may interfere in determining the tyrosine. Hence, simultaneous determination of DA and Tyrosine is highly essential in electrochemical analytical research.

Three electrode voltammetry was carried out for electrochemical characterization and sensing. The primary event that reveals the existence of dopamine is the oxidation of dopamine on the surface of GCE. Dopamine molecules are linked to the surface of modified GCE electrode, releasing $2H^+$ ions to generate dopamine-o-quinone. These ions are then identified on the GCE, resulting in a conspicuous anodic peak on the voltammogram. Similarly, tyrosine molecules also attached to the electrode surface and releases $1H^+$ ion producing the ketone derivative of tyrosine and these ions are detected and analysed by CV studies. Scheme. 1 depicts a graphical illustration of this phenomenon.

4.2.1 EIS

Electrochemical impedance experiments in 0.1 M KCl at its formal potential in the frequency range 100 kHz to 100 mHz with a 10mV amplitude were performed to examine the electrical characteristics of the prepared electrodes. A typical EIS response of bare GCE and GO-SnS_2 quantum dots/GCE are shown in Fig. 5. At the bare GCE, a partial semicircle with a virtually straight tail indicates electron transport resistance to the redox probe. On the GO-SnS_2 quantum dot/GCE, the semicircle does not appear, suggesting a lower barrier to electron transmission. This is due to the high conductivity of the graphene oxide-SnS_2 formed on the surface. As indicated by the enhanced electrode's impedance behaviour, GO-SnS_2 has been effectively adsorbed on the GCE surface. The modified electrode's resistance is lower than the bare graphite electrodes, which could be due to improved conductivity of the modified electrode [35–36]. The impedance charts match the behaviour of the CV.

4.2.2 Simultaneous detection of dopamine and tyrosine on *GO-SnS_2* modified electrode

Simultaneous detection studies of dopamine and tyrosine were given in Fig. 6. There are no peaks observed in bare glassy carbon electrode as seen in Fig. 6(a) and moreover in case of GO-SnS_2/GCE with analyte only tyrosine is showing Ipa (current) 0.0187mA at Epa (voltage) 0.782V which is given in Fig. 6(f). And in the third case simultaneous detection of tyrosine and dopamine was carried out using 100 µM Dopamine and 500µM of tyrosine in PBS buffer solution at pH 7 and is given in Fig. 6(e). The oxidation peaks of dopamine and tyrosine are very well separated and peaks appeared at 0.202 V with current 0.0257962 mA, and the peak at 0.7952 V with current 0.02579 mA correspond to dopamine and tyrosine respectively. Thus, the CV studies clearly showing the modified GO-SnS_2/GCE was successful in separating and distinguishing the analytes dopamine and tyrosine.

With precise redox behaviour of dopamine, GO-SnS_2/GCE demonstrated a three-fold increase in anodic peak current of 0.0362 mA. (Fig. 6d). These GO-SnS_2 dots, which boosted conductivity and surface area, are responsible for the better electrochemical current responsiveness.

To prove the surface area of GCE increases with modification with GO-SnS_2, the electroactive area of bare GCE, GO-SnS_2/GCE were determined and compared using CV technique as per the Randles-Sevik Eq. (37).

$i_p = (2.69 \times 10^5)\, n^{3/2}\, D^{1/2}\, v^{1/2}\, Ac$

The electrochemical areas calculated by using the equation are 0.112 cm^2 and 0.226 cm^2 for base GCE and GO-SnS_2/GCE respectively. As seen from the values the electroactive surface area increases nearly by 50% compared to that of bare GCE

4.2.3 Effect of scan rate on peak current of dopamine and tyrosine

Using cyclic voltammetry, the impact of changing the sweep rate for 100 M dopamine in 0.1 M PBS at pH 7 was examined (Fig. 7A). Different scan speeds ranging from 50 to 400 mV/s were used to record the CV profiles. Peak current rose with a minor positive shift in peak potential in the region of 50 to 400 mV/s, as seen in the graph. Ipa vs potential and Ipa vs square root of scan rate demonstrate a linear relationship with zero intercept as seen in the figure inset. The regression equation is expressed as Ipa = 2.9852 x + 0.03638 (R^2 = 0.99418). The Ipa increased linearly with scan rate and the corresponding regression equation is obtained as Ipa = 0.082 x + 0.01431(R^2 = 0.99172). All these results confirm the diffusion-controlled process controlling the overall kinetics.

The number of electrons 'n' was estimated using Laviron's equation, which is expressed as below [38]

Ip = nFQυ/4RT

In the above equation, Ip represents the anodic peak current (A), Q represents the charge associated with oxidation (C), υ is the scan rate (V s-1), R represents the gas constant (8.314 J K-1 mol-1), and T is the temperature (K). The value of n was calculated as 1.94, which equals 2, indicating that dopamine oxidation is a two-electron transfer process (scheme 1).

Cyclic voltammetry profiles were recorded to investigate the influence of scan rate on the electroactive surface of GO-SnS_2 /GCE, on tyrosine (500 µM) are shown in Fig. 7. (B). Using Randles – Sevcil equation, a plot of Ipa versus square root of scan rate (50 to 400 mV/s) shows excellent linearity with zero intercept, Ipa = 0.00403 x – 0.0059 with R^2 = 0.9945 suggesting the diffusion controlled process for the oxidation of tyrosine. The charge transfer coefficient for GO-SnS_2/GCE was found to be 0.492 and the theoretical value is 0.5, indicating that the adsorption of reactants of intermediates onto the modified sensor is diffusion controlled, sluggish and irreversible.

4.2.4 Effect of increasing concentration of dopamine and tyrosine at *GO-SnS_2/GCE*

Figure 8(A), Demonstrates the cyclic voltagrams of various concentrations of dopamine. With the increase in concentration of dopamine the anodic peak current increased linearly. The modified GO-SnS_2/GCE is found to be sensitive at low and high concentration of dopamine. As acknowledged in the literature at higher concentration of dopamine another reduction peak was observed at – 0.445 mV potential. Apart from the oxidation and reduction peaks of dopamine, the third peak due to leucodopaminechrome observed due to ring closure of dopamine-o-quinone [39, 40]. Effect of varying concentration of tyrosine at modified GO- GO-SnS_2/GCE is shown in Fig. 8(B) and a similar trend as seen in dopamine were observed. As prominent oxidation peak at 500µM is seen in tyrosine studies, this concentration was chosen for all the comparative studies.

4.2.5 Effect of pH on Dopamine and tyrosine studies

CV tests were performed to assess the influence of pH on oxidation of dopamine at PBS solutions with varying pH ranging from 4 to 12 at a scan rate of 50 mV/s to enhance the electrochemical responsiveness of the GO-SnS2/GCE towards the electrochemical oxidation of DA (Fig. 9A). The peak potential shifts to the negative side when pH rises from 4 to 11, owing to enhanced reversibility of the oxidation which involves deprotonation at elevated pH ranges (Fig. 9A). Furthermore, pH = 7 PBS had a superior electrochemical response in sensor applications. As a result, pH = 7 PBS was discovered to be optimal electrolyte for electrochemical research.

Effect of pH on tyrosine oxidation in PBS solutions with varying pH from 4–12 at a scan rate of 50 mV/s was given in Fig. 9(B). With increase in concentration there is increase in anodic peak current but the relative response was low when compared to dopamine. There is shift in negative peak potentials due to increase in reversibility of the oxidation at elevated pH of 7 and concentration of 500 µM was found to be optimum for tyrosine studies.

4.2.6 Chronoamperometric studies

In order to understand the response character of GO-SnS_2/GCE to dopamine chronoamperometry studies were carried out by successive addition of 50 μM dopamine at 25 sec time intervals in PBS solution containing 0.1M KCl is shown in Fig. 10. The response current was measured at fixed potential of + 0.25 V under stirring, for each addition of dopamine almost equal current steps were observed which indicates the efficient and catalytic activity of GO-SnS_2/GCE electrode. In the concentration range of 25 x 10 − 6 to 250 x 10 − 6 M, a linear connection between peak current and DA concentration was observed, with the lowest detection limit being 26 nM. Under ideal chronoamperometric circumstances, GO-SnS2 quantum dots/GCE were examined with additional co-existing interferences such as uric acid, ascorbic acid, and glucose and found no influence on the electrochemical oxidation of DA (figure not shown).

4.2.7 Stability and reproducibility of GO-SnS_2/ GCE electrode

The electrode's stability was tested by immersing it for three weeks in a phosphate buffer solution with a pH of 7.0. Every week, CVs were collected and compared to the ones received on the first day. The oxidation peak current was found to be somewhat lower than anticipated. The current reduction was just 10% after three weeks, indicating that the modified electrode is highly stable. The modified electrode's repeatability was tested ten times with 100 μM DA. After each measurement, the modified electrode was rinsed with buffer solution and evaluated for the same concentration. The enhanced electrode has an RSD (relative standard deviation) of 3.8 percent, showing that it is not vulnerable to surface fouling.

Conclusion

Finally, using a facile ultrasonication and hydrothermal method, the quantum dots of SnS_2-carbon composites were synthesized. The as synthesized materials were characterized by using various techniques like XRD, SEM, TEM, EDX and elemental mapping, XPS, and pore size distribution. These dots were used to construct a modified glassy carbon electrode for dopamine and tyrosine detection. For EIS, CV and chronoamperometric studies, the electrocatalytic activity of modified electrodes is investigated. Intriguingly, chronoamperometric studies discloses a LOD of 26 nM for dopamine detection. Compared to dopamine the relative response of tyrosine is less. The modified electrode has excellent stability, selectivity, sensitivity, and reproducibility, according to our research.

Declarations

Conflict of interest: The authors declare that they have no conflicts of interest.

References

1. J. Greenstein, M. Winitz, Chemistry of the amino acids. Yale J. Biol. Med. **38**, 383–384 (1966)
2. M.L. Heien, A.S. Khan, J.L. Ariansen, J.H. Cheer, P.E. Phillips, K.M. Wassum, R.M. Wightman, Real-time measurement of dopamine fluctuations after cocaine in the brain of behaving rats. Proc. Natl. Acad. Sci. USA 102, (2005) 10023–10028

3. T. Paus, Primate anterior cingulate cortex: Where motor control, drive and cognition interface. Nat. Rev. Neurosci. **2**, 417–424 (2001)
4. N.D. Volkow, G.-J. Wang, J.S. Fowler, D. Tomasi, F. Telang, Addiction: Beyond dopamine reward circuitry. Proc. Natl. Acad. Sci. USA, 108 (2011) 15037–15042
5. R.A. Wise, Dopamine, learning and motivation. Nat. Rev. Neurosci. **5**, 483–494 (2004)
6. R. Cools, Role of dopamine in the motivational and cognitive control of behavior. Neuroscientist **14**, 381–395 (2008)
7. S.R. Ali, Y. Ma, R.R. Parajuli, Y. Balogun, W.Y.-C. Lai, H.A. He, Nonoxidative sensor based on a self-doped polyaniline/carbon nanotube composite for sensitive and selective detection of the neurotransmitter dopamine. Anal. Chem. **79**, 2583–2587 (2007)
8. R.M. Wightman, L.J. May, A.C. Michael, Detection of dopamine dynamics in the brain. Anal. Chem. **60**, 769A–793A (1988)
9. M. Meyyappan, Nano biosensors for neurochemical monitoring. Nano Conv **2**, 18 (2015)
10. H.-C. Lee, T.-H. Chen, W.-L. Tseng, C.-H. Lin, Novel core etching technique of gold nanoparticles for colorimetric dopamine detection. Analyst **137**, 5352–5357 (2012)
11. T.H. Kim, C.H. Yea, S.T.D. Chueng, P.T.T. Yin, B. Conley, K. Dardir, Y. Pak, G.Y. Jung, J.W. .Choi, K.B.Lee, Large-scale nanoelectrode arrays to monitor the dopaminergic differentiation of human neural stem cells. Adv. Mater. **27**, 6356–6362 (2015)
12. K.E. Hubbard, A. Wells, T.S. Owens, M. Tagen, C.H. Fraga, C.F. Stewart, Determination of dopamine, serotonin, and their metabolites in pediatric cerebrospinal fluid by isocratic high performance liquid chromatography coupled with electrochemical detection. Biomed. Chromatogr. **24**, 626–631 (2010)
13. B. Kong, A. Zhu, Y. Luo, Y. Tian, Y. Yu, G. Shi, Sensitive and selective colorimetric visualization of cerebral dopamine based on double molecular recognition. Angew Chem. Int. Edit **123**, 1877–1880 (2011)
14. Y. Luo, L. Ma, X. Zhang, A.Z. Liang, Jiang, Sers detection of dopamine using label-free acridine red as molecular probe in reduced graphene oxide/silver nanotriangle sol substrate. Nanoscale Res. Lett. **10**, 230 (2015)
15. Y. L.Tang, Y. Wang, H. Li, J. Feng, J. Lu, Li, Preparation, structure, and electrochemical properties of reduced graphene sheet films. Adv. Funct. Mater. **19**, 2782–2789 (2009)
16. N.G. Shang, P. Papakonstantinou, M. McMullan, M. Chu, A. Stamboulis, A. Potenza, S.S. Dhesi, H. Marchetto, Catalyst-free efficient growth, orientation and biosensing properties of multilayer graphene nanoflake films with sharp edge planes. Adv. Funct. Mater. **18**, 3506–3514 (2008)
17. Y. Shao, J. Wang, H. Wu, J. Liu, I.A. Aksay, Y. Lin, Graphene based electrochemical sensors and biosensors: A review. Electroanalysis **22**, 1027–1036 (2010)
18. J. Ping, J. Wu, Y. Wang, Y. Ying, Simultaneous determination of ascorbic acid, dopamine and uric acid using high-performance screen-printed graphene electrode. Biosens. Bioelectron. **34**, 70–76 (2012)

19. Y. Mao, Y. Bao, S. Gan, F. Li, L. Niu, Electrochemical sensor for dopamine based on a novel graphene-molecular imprinted polymers composite recognition element. Biosens. Bioelectron. **28**, 291–297 (2011)
20. H. Kim, K.-Y. Park, J. Hong, K. Kang, All-graphene-battery: Bridging the gap between supercapacitors and lithium-ion batteries. Sci. Rep. **4**, 5278 (2014)
21. X. Miao, S. Tongay, M.K. Petterson, K. Berke, A.G. Rinzler, B.R. Appleton, A.F. Hebard, High efficiency graphene solar cells by chemical doping. Nano Lett. **12**, 2745–2750 (2012)
22. S.H. Chae, Y.H. Lee, Carbon nanotubes and graphene towards soft electronics. Nano Conv. **1**, 15 (2014)
23. S. Woo, Y.-R. Kim, T.D. Chung, Y. Piao, H. Kim, Synthesis of a graphene–carbon nanotube composite and its electrochemical sensing of hydrogen peroxide. Electrochim. Acta **59**, 509–514 (2012)
24. M. Mallesha, R. Manjunatha, C. Nethravathi, G.S. Suresh, J.S. Rajamathi,; Melo, T.V. Venkatesha, Functionalized-graphene modified graphite electrode for the selective determination of dopamine in presence of uric acid and ascorbic acid. Bioelectrochemistry **81**, 81, 104–108 (2011)
25. D. Li, M.B. Müller, S. Gilje, R.B. Kaner, G.G. Wallace, Processable aqueous dispersions of graphene nanosheets. Nat. Nanotechnol **3**, 101–105 (2008)
26. K. Wu, J. Fei, S. Hu, Simultaneous determination of dopamine and serotonin on a glassy carbon electrode coated with a film of carbon nanotubes. Anal. Biochem. **318**, 100–106 (2003)
27. L. Zhang, X. Jiang, Attachment of gold nanoparticles to glassy carbon electrode and its application for the voltammetric resolution of ascorbic acid and dopamine. J. Electroanal. Chem. **583**, 292–299 (2005)
28. C.-X. Xu, K.-J. Huang, Y. Fan, Z.-W. Wu, J. Li, T. Gan, Simultaneous electrochemical determination of dopamine and tryptophan using a TIO_2-graphene/poly(4-aminobenzenesulfonic acid) composite film based platform. Mater. Sci. Eng. C **32**, 969–974 (2012)
29. L. Jiang, Z. Fan, Design of advanced porous graphene materials: From graphene nanomesh to 3D architectures. Nanoscale **6**, 1922–1945 (2014)
30. K. Celebi, J. Buchheim, R.M. Wyss, A. Droudian, P. Gasser, I. Shorubalko, J.-I. Kye, C. Lee, H.G. Park, Ultimate permeation across atomically thin porous graphene. Science **344**, 289–292 (2014)
31. M. Dekun, Q. Tang, W. Zhang, Q. Tang, R. Zhang, W. Yu, Y. Zhou, J. Nanosci. Nanotechnol. **10**, 1–4 (2005)
32. H. Chen, B. Zhang, J. Zhang, W. Yu, J. Zheng, Z. Ding, H. Li, L. Ming, D.A. Mifounde Bengono, S. Chen, H. Tong, In-situ Grown SnS_2 Nanosheets on rGO as an Advanced Anode Material for Lithium and Sodium Ion Batteries Front. Chem., (2018) | https://doi.org/10.3389/fchem.2018.00629
33. A. Zhu, L. Qiao, Z. Jia, P. Tan, Y, liu, Y. maa, J. Pan**,** C-S bonds induced ultrafine SnS_2 dots/ porous g-C_3N_4 sheets 0D/2D heterojunction: synthesis and photocatalytic mechanism investigation**,** 46 (2017)17032 DOI:10.1039/C7DT03894A

34. M. Choia , W. Williamb , J. Hwanga , D. Yoona , J. Kima,b, A Supercritical Ethanol Route for One-pot Synthesis of Tin Sulfide–Reduced Graphene Oxides and Their Anode Performance for Lithium Ion BatteriesJournal of Industrial and Engineering Chemistry 59 (2018) 160–166
35. F. Huang, Y. Peng, G. Jin, S. Zhang, J. Kong, Selective determination of haloperidol and hydroxyzine at multi-walled carbon nanotubes-modified glassy carbon electrodes, Sensors 8 (2008) 1879–1889
36. R. Manjunatha, G.S. Suresh, J.S. Melo, F. Stanislaus D'SouzaT. Venkatarangaiah, Venkatesha, Simultaneous determination of ascorbic acid, dopamine and uric acid using
37. polystyrene sulfonate wrapped multiwalled carbon nanotubes bound to graphite electrode through layer-by-layer technique,Sensors and Actuators B: Chemical Volume 145, Issue 2, 19 March 2010, Pages 643–650
38. P. Zanello, "Inorganic Electrochemistry: Theory, Practice and Application" The Royal Society of Chemistry 2003. ISBN 0-85404-661-5
39. E. Laviron, General Expression of the Linear Potential Sweep Voltammogram in the Case of Diffusion less Electrochemical Systems. J. Electroanal. Chem. Interfacial. Electrochem. **101**, 19–28 (1979). https://doi.org/10.1016/S0022-0728(79)80075-3
40. H. Zhao, Y. Zhang, Z. Yuan, Electrochemical determination of dopamine using a poly(2-picolinic acid) modified glassy carbon electrode. Analyst **126**, 358–360 (2001)
41. G. Jin, Y. Zhang, W. Cheng, Poly (p-aminobenzene sulfonic acid)-modified glassy carbon electrode for simultaneous detection of dopamine and ascorbic acid. Sens. Actuators B **107**, 528–534 (2005)

Scheme

Schemes 1 is available in the Supplementary Files section.

Figures

Figure 1

X ray diffraction patterns of GO-SnS_2 quantum dots

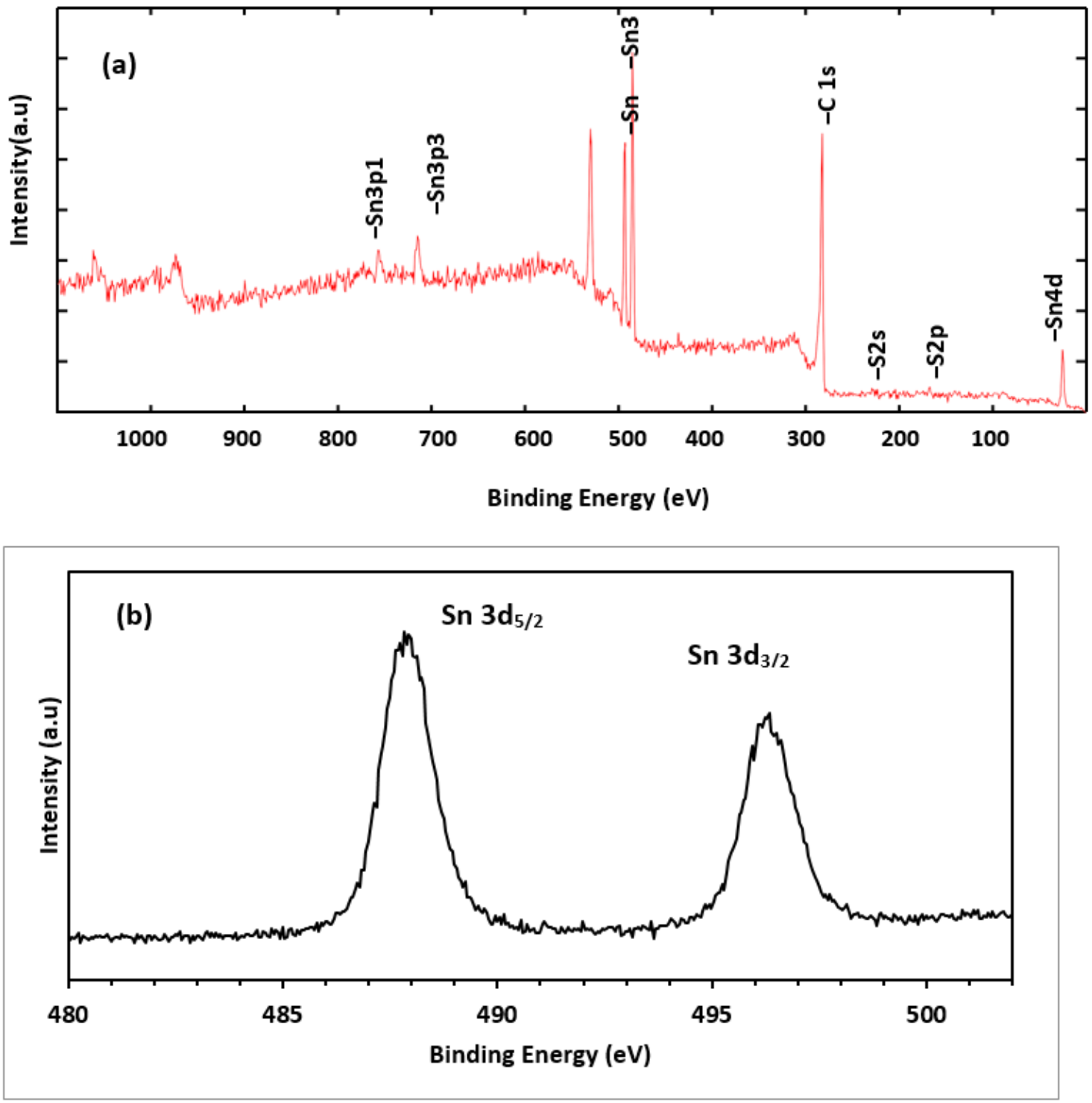

Figure 2

XPS spectra of the GO-SnS_2 quantum dots high resolution spectra of

a) Survey spectrum b) Sn 3d $_{5/2}$ and Sn 3d $_{3/2}$

Figure 3

Pore sized distribution of SnS_2-GO quantum dots (a) Pore diameter

(b) Surface area and (c) Pore volume

Figure 4

SEM and TEM images of as synthesized GO-SnS_2 quantum dots (a) SEM (b) TEM (c) EDAX and (d) SAED pattern

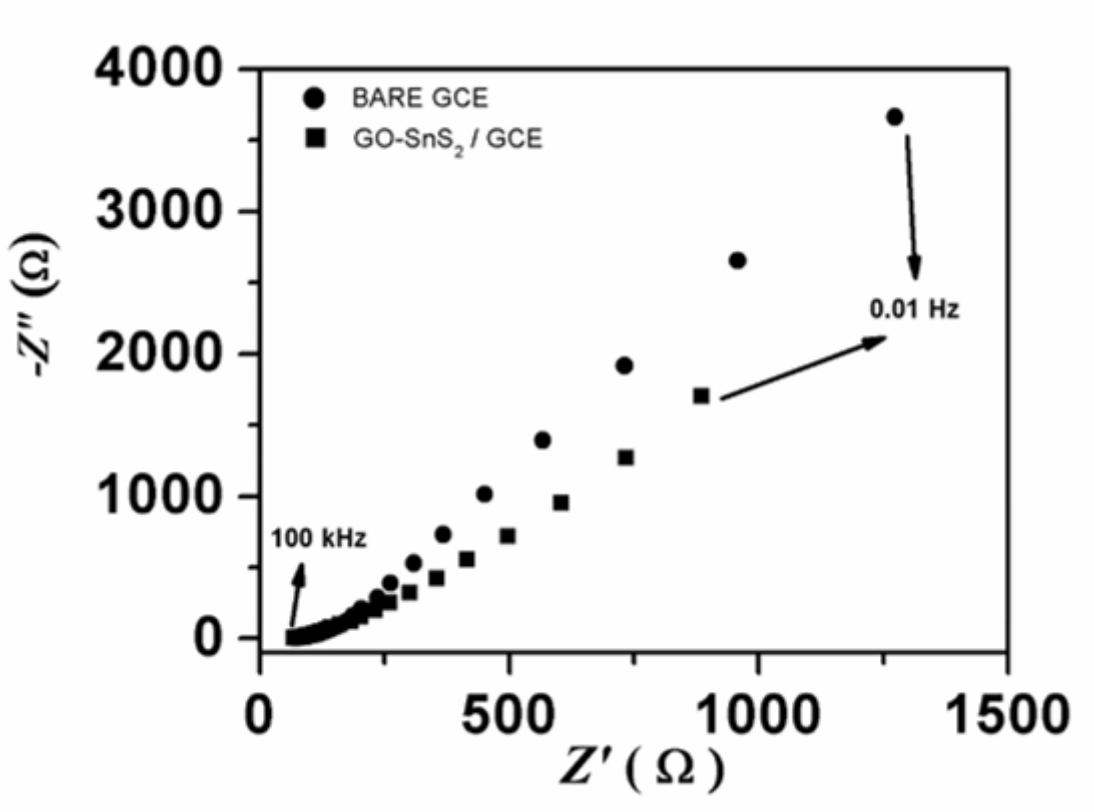

Figure 5

Nyquist impedance plots of bare GCE and GO-SnS_2 modified GCE in frequency range 100 kHz to 100mHz and the supporting electrolyte is 0.1 M KCl in 0.1 M PBS.

Figure 6

Simultaneous detection studies of Dopamine and tyrosine on GO-SnS_2 /GCE: a)bare GCE without any analyte, b) bare GCE with dopamine, c) GCE coated with GO-SnS_2 without analyte, d) GCE coated with GO-SnS_2 with dopamine, e) GO-SnS_2/GCE with dopamine 100μM + tyrosine 500 μM, f) GO-SnS_2/GCE with 500 μM tyrosine at scan rate of 50mvs.

Figure 7

Cyclic voltagrams recorded at different scan rates using (A) 100 μM dopamine and (B) 500μM tyrosine at SnS_2-GO/GCE in 0.1 M PBS solution of pH 7: a) 50, b) 100, c)150, d)200 e)300, f) 400 mV

Figure 8

Cyclic voltagrams recorded at varying concentration at GO-SnS_2/GCE in PBS solution of pH 7of (A) dopamine (a-h): a) 25, b) 50, c)75, d) 100, e) 125, f) 150, g) 200, h) 250 μM and (B) Tyrosine: a) 25, b) 50, c) 100, d) 200, e) 300, f) 400, g) 500 μM at 50 mV/s

Figure 9

Cyclic voltagrams of (A) 100μM dopamine and (B) 500μM tyrosine with varying pH using 0.1 M PBS, scan rate 50mV: (a-i); a)4, b)5, c)6, d)7, e)8, f)9, g)10, h)11, i)12

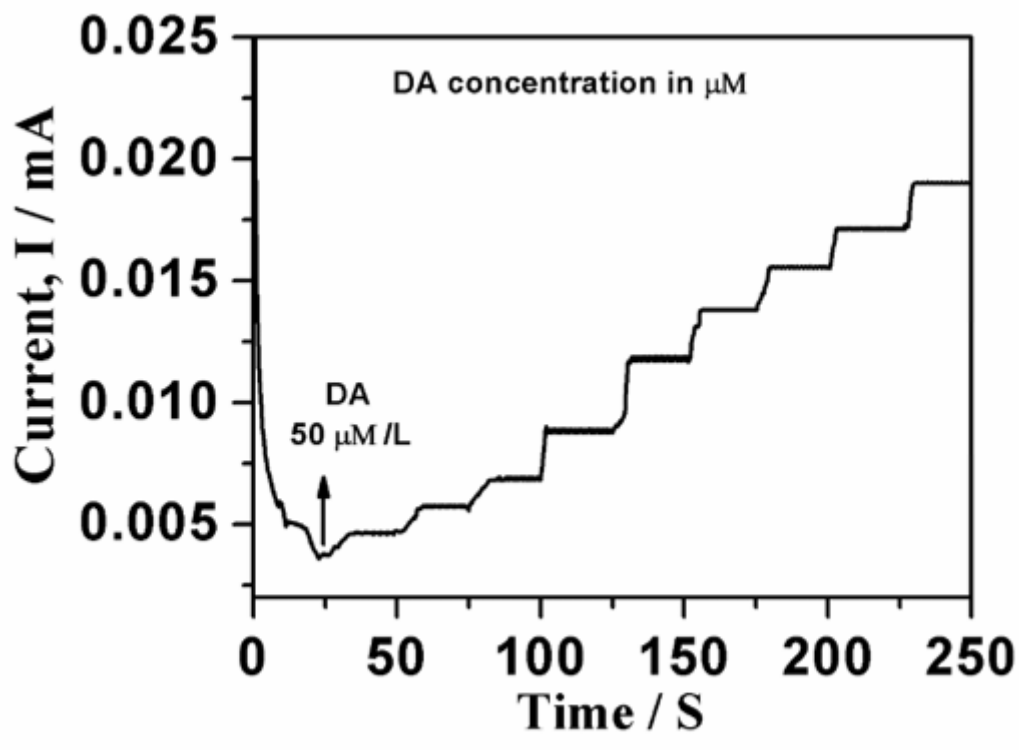

Figure 10

Amperometry response of GO-SnS_2/ GCE for each addition of 50 μM DA at constant applied potential of + 0.25 V in PBS containing 0.1 M KCl (pH 7.0)

Supplementary Files

This is a list of supplementary files associated with this preprint. Click to download.

- Scheme1.png